Available online at www.sciencedirect.com
SCIENCE DIRECT
Polymer 45 (2004) 5913–5921
polymer
www.elsevier.com/locate/polymer

Thermal properties, miscibility and specific interactions in comparison of linear and star poly(methyl methacrylate) blend with phenolic

Chih-Feng Huang[a], Shiao-Wei Kuo[a], Han-Ching Lin[a], Jem-Kun Chen[a], Yu-Kai Chen[a], Hongyao Xu[b], Feng-Chih Chang[a,*]

[a]*Institute of Applied Chemistry, National Chiao Tung University, Hsin Chu 30050, Taiwan, ROC*
[b]*Department of Chemistry, Anhui University, Anhui, 230039, China*

Received 4 February 2004; received in revised form 12 April 2004; accepted 18 May 2004

Abstract

A series of miscible linear and star poly(methyl methacrylate) (PMMA)/phenolic blends with different compositions have been prepared. T_gs of both systems are negative derivation from the average values, implying that the self-association interaction is stronger than the inter-association interaction between linear or star PMMA with phenolic. The proton spin–lattice relaxation time in the rotating frame ($T_{1\rho}^H$) determined by high resolution solid state ^{13}C NMR indicates single composition dependent $T_{1\rho}^H$ from all blends, implying a good miscibility with chain dynamics on a scale of 1–2 nm. However, $T_{1\rho}^H$s of star PMMA/phenolic blends are relatively smaller than those of linear PMMA/phenolic blends, implying that the degree of homogeneity of star PMMA/phenolic blends is higher than those of linear PMMA/phenolic blends. According to FT-IR analyses, the above results can be rationalized that the hydrogen-bonding interaction of the star PMMA/phenolic blends is greater than the corresponding linear PMMA/phenolic blends.

Keywords: Hydrogen bond; Polymer blend; Star polymer

1. Introduction

Miscible polymer blends and the strong interaction provide attractive interest in polymer science due to their strong economic incentives arising from their potential application. It has been demonstrated that poly(methyl methacrylate) (PMMA) is able to interact with polymers of a wide variety of structures, such as poly(vinyl phenol) [1], phenoxy [2], poly(ethylene oxide) [3], and poly(vinylidene fluoride) [4]. In blends of two polymer chains, the bulk thermodynamic interaction can vary with blend composition, microstructure [5], tacticity [6], and isotopic labeling [7,8]. Branched polymer architectures, such as hyperbranched polymers and star polymers have received great attention in recent year [9,10], because they posses a special structure, with greater number of terminal groups and physical properties different from their linear analogs, such as high solubility and low melt viscosity. Although the effects of branching in polymers have long been recognized as an important area of study [11,12], the ability to control branching architecture has only recently been achieved. Over the past two decades, dramatic advances in polymer syntheses have provided a means to control polymer architecture on the molecular length scale, thus allowing the creation of a variety of novel macromolecules and the opportunity to experimentally investigate the effects of polymer architecture. The strength and extent of polymer interaction is typically expressed in terms of effective segment–segment-interaction parameter, χ_{eff}, which varies with all these molecular particulars. The fluctuation theory of Fredrickson et al. [13] suggests that if one component in a polymer blend is a long-chain branched architecture, the bulk interaction will affect the case of an analogous blend with linear components. This influence in the bulk interaction should manifest itself in an architectural contribution to the value of the χ_{eff} parameter, although the architectural effect is intrinsically a non-local effect.

In our previous works [14–16], we studied the miscibility and the specific polymer–polymer interactions based on linear analogs. Recently, a new synthetic method of well-defined branched polymers has been developed [17].

* Corresponding author. Tel.: +886-3-5727077; fax: +886-3-5719507.
E-mail address: kuosw@cc.nctu.edu.tw (F.C. Chang).

0032-3861/$ - see front matter © 2004 Elsevier Ltd. All rights reserved.
doi:10.1016/j.polymer.2004.05.043

In this paper, star and linear PMMA were prepared by atom transfer radical polymerization (ATRP) [18] and then blended with phenolic resin. We intend to compare the miscibility and specific interactions between star and linear PMMA. Characterizations were carried out using gel permeation chromatography (GPC), differential scanning calorimetry (DSC), Fourier transform infrared spectroscopy (FT-IR), and high-resolution solid-state ^{13}C nuclear magnetic resonance (NMR) spectroscopy.

2. Experimental

2.1. Materials and syntheses

The 4-arm initiator was synthesized as described in our previous paper [18]. To prepare the 4-arm star PMMA, the ATRP with CuBr/*N*,*N*,*N*′,*N*″,*N*″-pentamethyldiethylenetriamine (PMDETA) was carried out. The molecular weight (Mn = 95,000g/mol) was determined by GPC. In accordance with the controlled polymerization characteristics of ATRP, the polydispersity of this star PMMA is low (PDI = 1.21). The linear analog of the PMMA polymer was also prepared by ATRP with methyl DL-2-bromopropionate monofunctional initiator. The molecular weight (M_n = 100,000 g/mol) was also determined by GPC and the polydispersity of this linear PMMA is 1.18. The phenolic was synthesized with sulfuric acid via a condensation reaction and with average molecular weights of M_n = 500 and M_w = 1200 that was described in the previous study [19]. The chemical structure of the Novolac-type phenolic resin consists of phenolic rings bridge-linked randomly by methylene groups with 19% *ortho–ortho*, 57% *ortho–para*, and 24% *para–para* methylene bridges, identified by the solution ^{13}C NMR spectrum. The phenolic resin does not contain any reactive methylene group, which is capable of causing cross-linking on heating. The chemical structures of PMMA and phenolic resin are shown as follows in Scheme 1.

2.2. Blend preparation

Desired composition containing star or linear PMMA and phenolic was dissolved in THF at a concentration of 5 wt% and stirred for 6–8 h. The solution was allowed to evaporate slowly at 25 °C for 1 day on a Teflon plate and dried at 90 °C for 3 days to ensure total elimination of the solvent.

2.3. Differential scanning calorimetry (DSC)

Thermal analysis was carried out on a DSC instrument from DuPont (model 910 DSC-9000 controller) with a scan rate of 20 °C/min and a temperature range of 30–170 °C in nitrogen atmosphere. Approximately 5–10 mg sample was weighted and sealed in an aluminum pan. The sample was then quickly cooled to room temperature from the first scan and then scanned between 30 and 280 °C at a scan rate of 20 °C/min. The glass transition temperature is taken as the midpoint of the heat capacity transition between the upper and lower points of deviation from the extrapolated glass and liquid lines.

2.4. FT-IR spectra

FT-IR measurement was made using a Nicolet Avatar 320 FT-IR Spectrometer, 32 scans at a resolution of 1 cm^{-1} were collected with a NaCl disk. The THF solution containing the sample was cast onto a NaCl disk and dried under condition similar to that used in bulk preparation. The sample chamber was purged with nitrogen in order to maintain the film dryness.

2.5. Solid-state NMR

High-resolution solid-state ^{13}C NMR experiments were carried out at 25 °C using a Bruker DSX-400 Spectrometer operating at a resonance frequency of 100.47 MHz for ^{13}C. The high-resolution solid-state ^{13}C NMR spectra were acquired by using the cross-polarization (CP)/magic angle spinning (MAS)/high-power dipolar decoupling (DD) technique. A 90° pulse width of 3.9 μs with 3 s pulse delay time and an acquisition time of 30 ms with 2048 scans were used. A magic angle sample-spinning rate of 5.4 KHz was used to avoid absorption overlapping. The proton spin–lattice relaxation time in the rotating frame ($T_{1\rho}^{H}$) was determined indirectly via carbon observation using a 90° − τ-spin lock pulse sequence prior to CP. The data acquisition was performed at a delay time (τ) ranging from 0.1 to 12 ms with a contact time of 1.0 ms.

3. Results and discussion

3.1. DSC analyses

In general, the DSC analysis is one of the most convenient methods to determine the miscibility in polymer blends. The glass transition temperatures of these pure polymers synthesized in this study, PMMA and phenolic, are 104 and 50 °C, respectively. Fig. 1 shows the conventional second run DSC thermograms of these homopolymers and linear or star PMMA/phenolic blends with various weight ratios (10/90, 30/70, 50/50, 70/30, 90/10). Essential all these blends have a single T_g. A single T_g strongly suggests that these blends are fully miscible with domain dimension on the order of 20–40 nm. Essentially, all T_gs are below the liner relationship of mother polymers. Generally, if T_g-composition relationship is negative deviation, neither a linear relationship nor the ideal rule of Fox is applicable [20]. The Godon–Taylor equation describes the T_g relationship for most polymer mixtures

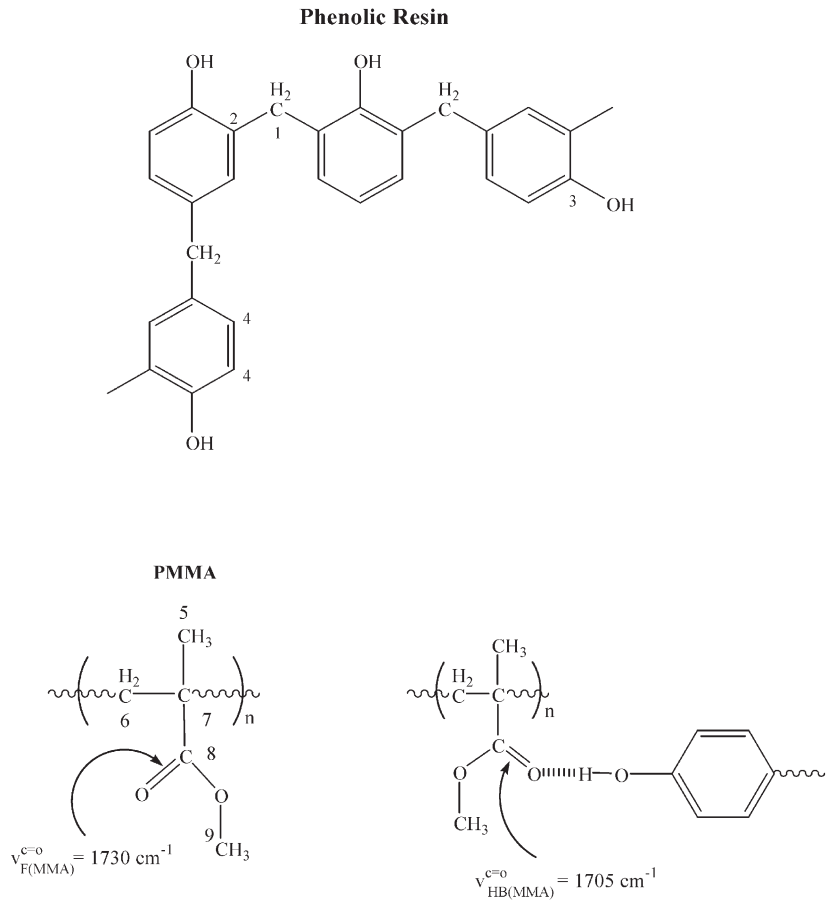

Scheme 1. Schematic diagram showing carbon number and type of interaction between PMMA and phenolic.

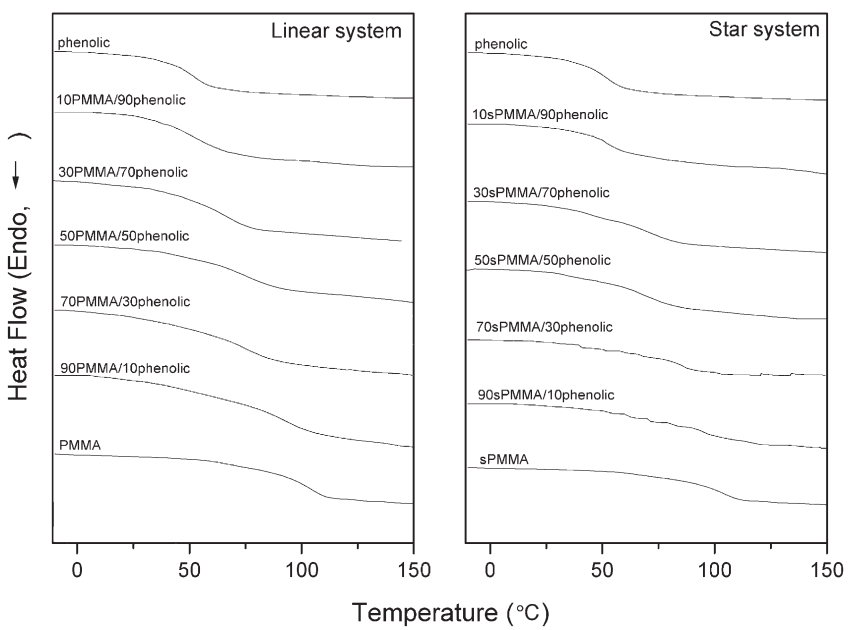

Fig. 1. DSC thermograms of the linear or star PMMA/phenolic blends with different compositions (weight ratio).

with good molecular-scale mixing without aggregation or specific interaction. To quantitatively assess the degree of interactions between PMMA and phenolic segments, the Kwei equation is the most popular equation to predict the variation of glass transition temperature [21] by the following T_g-composition relationship:

$$T_g = \frac{W_1 T_{g1} + kW_2 T_{g2}}{W_1 + kW_2} + qW_1 W_2 \quad (1)$$

where W_1 and W_2 are weight fractions of compositions, T_{g1} and T_{g2} represent the corresponding glass transition temperatures, k and q are fitting constants. As shown in Fig. 2 curve (b), $k = 1$ and $q = -17$ are obtained from the non-linear least squares 'best fit' values [22] for the star PMMA/phenolic blend system. The q is a parameter corresponding to the strength of hydrogen bonding in the blend, reflecting a balance between the breaking of the self-association and the forming of the inter-association hydrogen bonding. Comparing with the $k = 1$ and $q = -32$ of the linear PMMA/phenolic blend system (Fig. 2 curve (c)), the inter-association hydrogen-bonding interaction of the star PMMA/phenolic blends is stronger than the linear ones. In both linear and star blend systems, negative q were obtained, implying that the self-association interaction is stronger than the inter-association interaction between linear or star PMMA with phenolic blends.

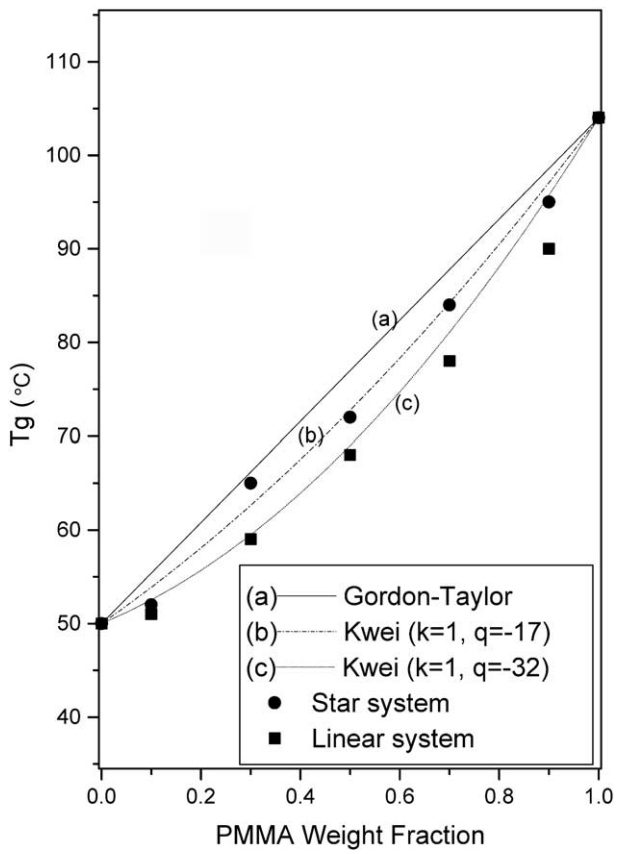

Fig. 2. T_g vs. composition curves based on (a) the Gordon–Taylor equation (b) the Kwei equation for star system (c) the Kwei equation for linear system (●) experimental data of star blends (■) experimental data of linear blends.

3.2. FT-IR spectra

Chemical structures of PMMA and phenolic are shown in Scheme 1, containing IR carbonyl vibrations from the free and hydrogen-bonded of PMMA with phenolic. The phenolic unit may exist as free state, self-associated dimmer, or inter-association with PMMA. For the MMA unit, the IR carbonyl stretching absorptions by free and hydrogen-bonded carbonyl groups are at 1730 and 1705 cm^{-1}, respectively [22]. Hence, states of PMMA and phenolic associations in these blends can be analyzed by FT-IR spectra. Fig. 3 shows the scale-expanded infrared spectra in the hydroxyl-stretching region with various compositions of linear and star PMMA/phenolic blends at room temperature. The spectra of the pure phenolic shows a broad band at 3350 cm^{-1} and a shoulder at 3525 cm^{-1}, corresponding to the multimer hydrogen-bonded (self-associated) hydroxyl groups and the free hydroxyl groups, respectively. The intensity of the free hydroxyl bands both decreases with the increase of the linear or star PMMA content in these blends. It is expected that large portion of these 'free' OH groups is consumed by forming the inter-association hydrogen bonds between the PMMA and the phenolic. Meanwhile, the band (at about 3420 cm^{-1}), appears with the increase of the PMMA content as the result of the decrease in the free hydroxyl band. In addition, portion of the self-association hydrogen bends (at 3350 cm^{-1}) are broken off to form the inter-association hydrogen bends [23]. This phenomenon depicts that a new distribution of hydrogen bonding formation resulting from the competition between hydroxyl–hydroxyl and hydroxyl–carbonyl interactions. Coleman et al. [24] have used the frequency difference ($\Delta\nu$) between the hydrogen-bonded hydroxyl absorption and free hydroxyl absorption to access the average strength of the intermolecular interaction. Therefore, the hydroxyl–hydroxyl self-interaction is stronger than the hydroxyl–carbonyl inter-association from Fig. 3 for both linear and star PMMA/phenolic blends. These results are in agreement with the negative q value obtained from the Kwei equation.

Fig. 4 shows the infrared spectra of the carbonyl stretching measured at room temperature ranging from 1675 to 1765 cm^{-1} for different compositions of the linear and the star PMMA/phenolic blends. It clearly shows that the fraction of hydrogen bonded carbonyl in the star PMMA system is greater than that of linear system as shown in Fig. 4. By quantitative measuring the absorptivity ratio of the hydrogen bonded to the free carbonyl bands in a blend system, we can determine the fraction of hydrogen bonded carbonyl of the PMMA by using the $a_R = a_{HB}/a_F = 1.5$ [25,26]. Through least-squares curve-fitting within the carbonyl stretching region using four Gaussian bands. The parameters of the infrared carbonyl band are summarized in

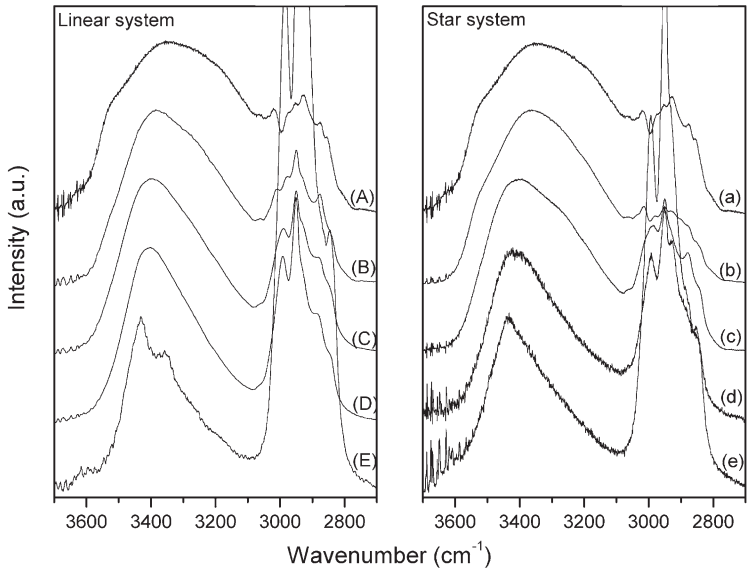

Fig. 3. FT-IR spectra recorded at room temperature in the 2700–3700 cm^{-1} region for various compositions (weight ratio) of linear and star PMMA/phenolic blends—linear system (left): (A) 10PMMA/90phenolic (B) 30PMMA/70phenolic (C) 50PMMA/50phenolic (D) 70PMMA/30phenolic (E) 90PMMA/10-phenolic; star system (right): (a) 10sPMMA/90phenolic (b) 30sPMMA/70phenolic (c) 50sPMMA/50phenolic (d) 70sPMMA/30phenolic (e) 90sPMMA/10-phenolic.

Table 1, where the hydrogen bonded carbonyl fraction of linear or star PMMA increases with the increase of the phenolic content. Fig. 5 plots the fraction of hydrogen bonded carbonyl from linear or star PMMA vs. the phenolic weight fraction of these two blend systems. According to the Painter–Coleman association model PCAM [23], we can determine the values of equilibrium constants describing the self-association, inter-association and other thermodynamic properties. The self-association equilibrium constants, K_2 and K_B corresponding to the hydroxyl–hydroxyl interaction of phenolic, represent the formation of hydrogen-bonded 'dimer' and 'multimer'. Apparently, a more suitable value of K_A is 25 for star PMMA/phenolic and 16 for linear PMMA/phenolic blend in this study based on the experimental data and theoretical prediction. Calculating the inter-association equilibrium constants followed a least square method has been widely discussed in our previous study [16]. Table 2 lists all the parameters required by the Painter–Coleman association model to estimate thermodynamic properties for these polymer blends. Clearly, the

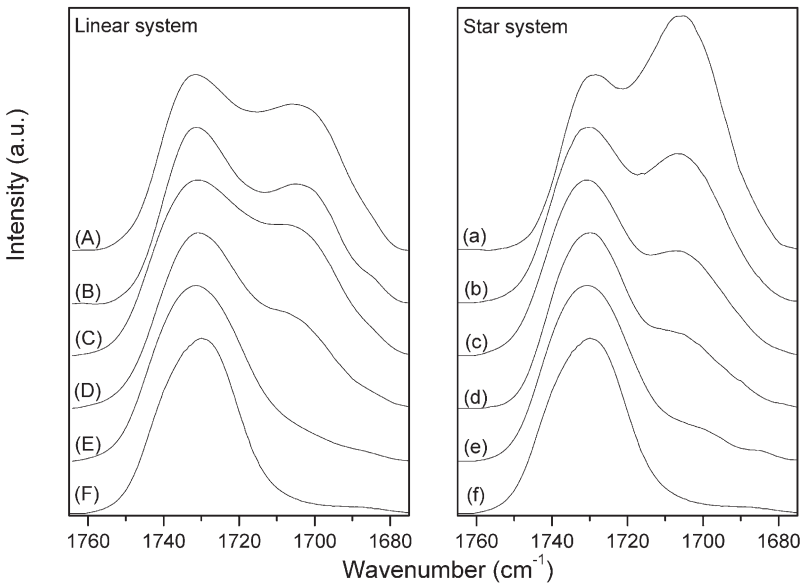

Fig. 4. FT-IR spectra recorded at room temperature in the 1675–1765 cm^{-1} region for various compositions (weight ratio) of the linear and star PMMA/phenolic blends—linear system (left): (A) 10PMMA/90phenolic (B) 30PMMA/70phenolic (C) 50PMMA/50phenolic (D) 70PMMA/30phenolic (E) 90PMMA/10phenolic (F) PMMA; star system (right): (a) 10sPMMA/90phenolic (b) 30sPMMA/70phenolic (c) 50sPMMA/50phenolic (d) 70sPMMA/30-phenolic (e) 90sPMMA/10phenolic (f) sPMMA.

Table 1
Carbonyl group curve-fitting results of the PMMA or sPMMA/phenolic blends

Samples (wt%)	Free C=O		H-bonded C=O		Fb[a] (%)
	ν_f (cm^{-1})	A_f (%)	ν_b (cm^{-1})	A_b (%)	
90MMA/10phenolic	1730.2	86.4	1705.1	13.6	9.5
70MMA/30phenolic	1731.1	71.1	1705.4	28.9	21.3
50MMA/50phenolic	1731.4	59.3	1705.3	40.7	31.4
30MMA/70phenolic	1731.5	50.8	1705.6	49.2	39.2
10MMA/90phenolic	1731.4	42.0	1705.5	58.0	47.9
Pure PMMA	1730.3	–	–	–	–
90sMMA/10phenolic	1731.5	84.4	1705.6	15.6	11.3
70sMMA/30phenolic	1731.3	65.5	1705.2	34.5	26.4
50sMMA/50phenolic	1731.7	56.4	1705.5	43.6	34.1
30sMMA/70phenolic	1731.4	43.9	1705.8	56.1	45.8
10sMMA/90phenolic	1730.3	29.0	1705.9	71.0	62.3

ν_f : wavenumber of free C=O of PMMA; ν_b : wavenumber of hydrogen bonded carbonyl of PMMA; A_f : free C=O area fraction of PMMA; A_b : C=O area fraction of hydrogen bonded PMMA.
[a] fb: fraction of hydrogen bonded PMMA $= (A_b/1.5)/(A_b/1.5 + A_f)$.

Table 2
Summary of the self-association and inter-association equilibrium constants and thermodynamic parameter of star PMMA/phenolic and linear PMMA/phenolic blends at 25 °C

Polymer	V	M_w	δ	DP	Equilibrium constant		
					K_2	K_B	K_A
Phenolic[a]	84	105	12.05	6	23.3	52.3	–
SPMMA[b]	84.9	100	9.1	900	–	–	25
PMMA[b]	84.9	100	9.1	1000	–	–	16

V : molar volume (ml/mol), M_w : molecular weight (g/mol), δ : solubility parameter $(cal/ml)^{1/2}$, DP: degree of polymerization, K_2 : dimmer self-association equilibrium constant, K_B : multimer self-association equilibrium constant, K_A : inter-association equilibrium constant.
[a] Ref. [14].
[b] Ref. [23].

inter-association equilibrium constant and relative ratio of K_A/K_B of hydrogen bonding donor group is in the order of star PMMA/phenolic blend > linear PMMA/phenolic blend.

3.3. Solid-state NMR analyses

Solid-state NMR spectroscopy has been used to better understand the phase behavior and miscibility of polymer blends. Fig. 6 shows the selected ^{13}C CP/MAS spectra of various linear and star PMMA/phenolic blends. Peak structural assignments (see Scheme 1) of ^{13}C CP/MAS spectra of PMMA and phenolic are shown in Fig. 6. Fig. 7 shows the carbonyl resonance of the PMMA (180 ppm) and the phenolic C-2 resonance (152 ppm) against the phenolic content. The chemical shifts of hydroxyl (C-2) from the phenolic and the carbonyl from the star PMMA in star PMMA/phenolic blends are greater than those from the corresponding linear PMMA/phenolic blends, suggesting that the hydrogen bonding strength within the star PMMA/phenolic blend is stronger than the corresponding linear blends. This result is also consistent with the observed glass transition temperature difference between star PMMA/phenolic and linear PMMA/phenolic blends.

A single T_g based on DSC analysis implies that the mixing of two blending components is in a scale of about 20–40 nm. The dimension of mixing smaller than 20 nm can be obtained through measurement of the spin–lattice relaxation time in the rotating frame ($T^H_{1\rho}$). The magnetization of resonance is expected to decay according to the

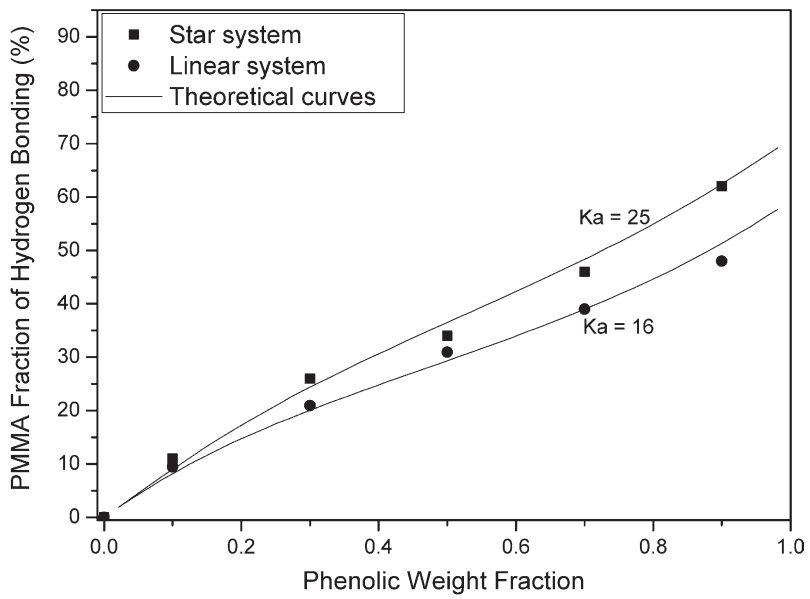

Fig. 5. Linear and star PMMA fraction of hydrogen bonded carbonyl vs. phenolic content for blends from FT-IR spectra.

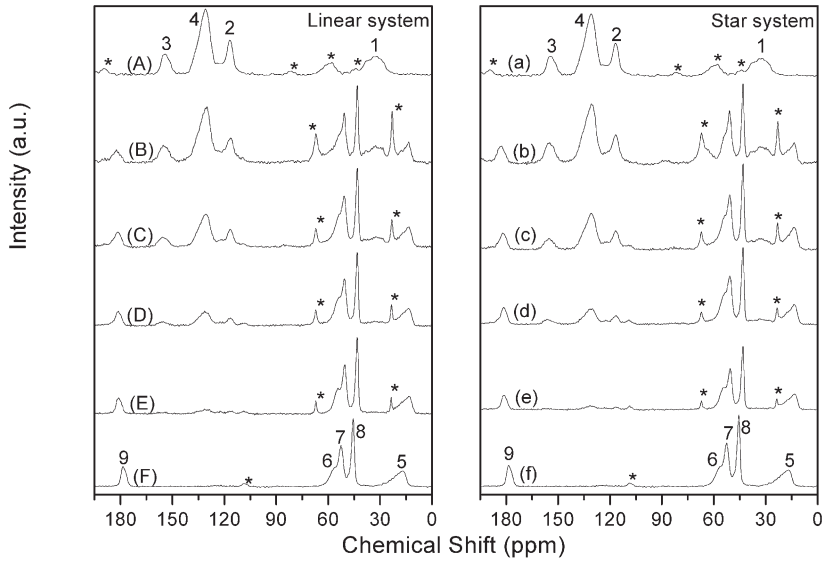

Fig. 6. ^{13}C CP/MAS NMR of the linear and star PMMA/phenolic blends at room temperature for various compositions (weight ratio) of the linear and star PMMA/phenolic blends—linear system (left): (A) phenolic (B) 30PMMA/70phenolic (C) 50PMMA/50phenolic (D) 70PMMA/30phenolic (E) 90PMMA/10phenolic (F) PMMA; star system (right): (a) phenolic (b) 30sPMMA/70phenolic (c) 50sPMMA/50phenolic (d) 70sPMMA/30phenolic (e) 90sPMMA/10phenolic (f) sPMMA.

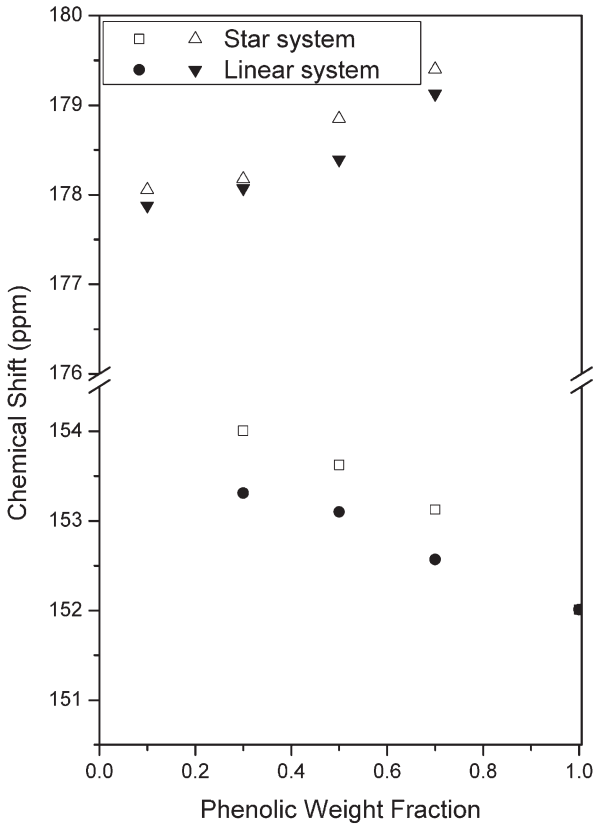

Fig. 7. ^{13}C CP/MAS NMR Chemical shift of 180 and 152 ppm with different phenolic content.

following exponential function model by Eq. (2) by the spin-locking mode employed in this study.

$$\ln(M_\tau/M_0) = -\tau/T_{1\rho}^H \quad (2)$$

where $T_{1\rho}^H$ is the spin–lattice relaxation time in the rotating frame, τ is the delay time used in the experiment, and M_τ is the corresponding resonance. $T_{1\rho}^H$ can be obtained from the slope of $\ln(M_\tau/M_0)$ vs. τ. Fig. 8 shows plots of $\ln(M_\tau/M_0)$ vs. τ. Quantitative analysis based on the phenolic C-2 resonance (152 ppm) is used to estimate homogeneities of these polymer blends. Linear relationship shown in Fig. 8 is in good agreement with Eq. (2). From the slope of the fitting line, the $T_{1\rho}^H$ value can be determined.

A single composition-dependent $T_{1\rho}^H$ is obtained for all PMMA/phenolic blends, suggesting that both blends are homogeneous to a scale where the spin-diffusion occurs within the time $T_{1\rho}^H$. The upper spatial scale of the spin-diffusion path length L can be estimated from the following

Table 3
$T_{1\rho}^H$ values and domain sizes for linear and star PMMA/phenolic blend

Samples (phenolic[a] wt%)	Linear system		Star system	
	$T_{1\rho}^H$ (ms)	Domain size (nm)	$T_{1\rho}^H$ (ms)	Domain size (nm)
10phenolic	14.56	2.09	13.32	2.00
30phenolic	10.10	1.74	9.03	1.65
50phenolic	6.94	1.44	6.25	1.37
70phenolic	4.80	1.20	4.10	1.11
90phenolic	3.66	1.05	–	–

[a] Pure phenolic: $T_{1\rho}^H = 5.65$ *ms*; domain size = 1.30 nm.

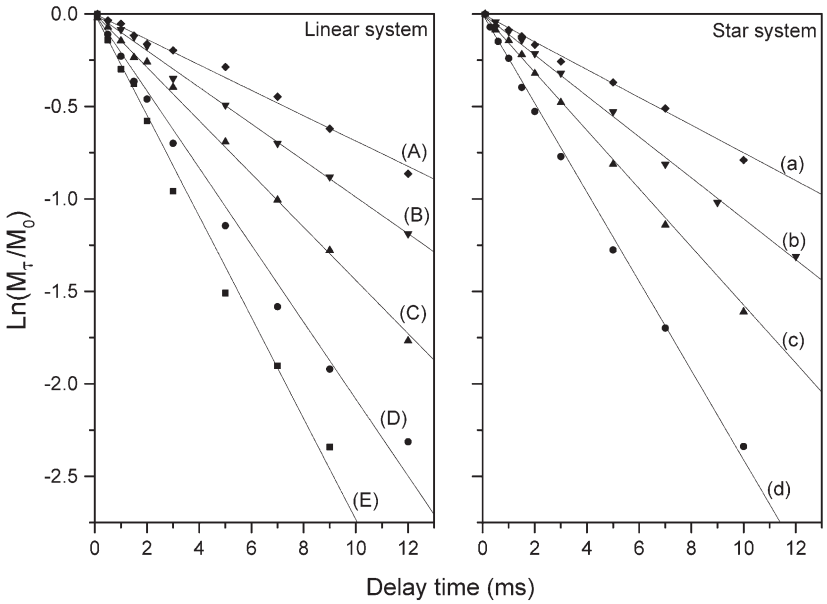

Fig. 8. Semi-logarithmic plots of the magnetization intensities of 116 ppm vs. delay time for linear and star PMMA/phenolic blends with a contact time of 1.0 ms—linear system (left): (A) 10PMMA/90phenolic (B) 30PMMA/70phenolic (C) 50PMMA/50phenolic (D) 70PMMA/30phenolic (E) 90PMMA/10-phenolic; star system (right): (a) 30sPMMA/70phenolic (b) 50sPMMA/50phenolic (c) 70sPMMA/30phenolic (d) 90sPMMA/10phenolic.

expression [27–29]:

$$L = (6DT_{1\rho}^{H})^{1/2} \tag{3}$$

where D, which is typically assumed to be 10^{-16} m^2s^{-1}, an effective spin-diffusion coefficient depending on the average proton to proton distance as well as the dipolar interaction. Hence, the upper spatial scales of the domain sizes are estimated to be 1–2 nm for these linear and star PMMA/phenolic blends as shown in Table 3. It can be seen that the star PMMA/phenolic blend system has relatively smaller domain sizes than the corresponding linear PMMA/phenolic blend system, indicating that the degrees of homogeneity of star blend system are relatively higher than those of linear blends. The star blend system, in general, has greater fraction of the hydrogen bonded carbonyl than the corresponding linear polymer blend due to the smaller radius of gyration of the former [30].

4. Conclusions

Linear and star PMMA/phenolic blends were investigated by using FT-IR, DSC, and high-resolution solid-state ^{13}C NMR. All these blends are totally miscible in the amorphous phase over entire compositions. The T_g of the star PMMA/phenolic blend is higher than that of the linear ones, both with negative q value. This result indicates that the self-association interaction is stronger than the inter-association interaction between blends of linear or star PMMA with phenolic. Measurements of $T_{1\rho}^{H}$ reveal that all blends possess single composition-dependent $T_{1\rho}^{H}$, indicating a good miscibility and chain dynamic on a scale of 2 nm or less. However, the $T_{1\rho}^{H}$ of the star PMMA/phenolic blend is relatively smaller than the corresponding linear PMMA/-phenolic blend, implying that the degree of homogeneity of the star blend system is higher than that of the linear blend due to higher miscibility of the star polymer. Better homogeneity of the star polymer blend can also be rationalized in terms of extent of hydrogen-bonding interaction, the fraction of the hydrogen bonded carbonyl from PMMA of star polymer is greater than the linear polymer based on FT-IR analyses.

Acknowledgements

This research was financially supported by the National Science Council, Taiwan, Republic of China, under Contract Nos. NSC-92-2216-E-009-018.

References

[1] Li D, Brisson J. Macromolecules 1996;29:868.
[2] Iriarte M, Alberdi M, Shenoy SL, Iruin JJ. Macromolecules 1999;32:2661.
[3] Dionisio M, Fernandes AC, Mano JF, et al. Macromolecules 2000;33:1002.
[4] Aihara T, Saito H, Inoue T, et al. Polymer 1998;39:129.
[5] Sakurai S, Jinnai H, Hasegawa H, Hashimoto T, Glen Hargis I, Aggarwal SL, Han CC. Macromolecules 1990;23:451.
[6] Beaucage G, Stein RS, Hashimoto T, Hasegawa H. Macromolecules 1991;24:3443.
[7] Graessley WW, Krishnamoorti R, Balsara NP, Fetters LJ, Lohse DJ, Schultz DN, Sissano JA. Macromolecules 1993;26:1137.
[8] Hopkinson I, Kiff FT, Richards RW, King SM, Munro H. Polymer 1994;35:1722.

[9] Tomalia DA, Nayor AM, Goddard WA. Angew Chem Int Ed Engl 1990;29:138.
[10] Kim YH. J Polym Sci Part A: Polym Chem 1998;36:1685.
[11] Zimm BH, Stockmayer WH. J Chem Phys 1949;17:1301.
[12] Flory PJ. Principles of polymer chemistry. Ithaca, NY: Cornell University Press; 1953.
[13] Fredrickson GH, Liu A, Bates FS. Macromolecules 1994;27:2503.
[14] Wu HD, Chu PP, Ma CCM, Chang FC. Macromolecules 1999;32: 3097.
[15] Kuo SW, Chang FC. Macromolecules 2001;34:5224.
[16] Kuo SW, Liu WP, Chang FC. Macromolecules 2003;36:6653.
[17] Patten TE, Matyjaszewski K. Acc Chem Res 1999;32:895.
[18] Huang CF, Kuo SW, Lee HF, Xu HY, Chang FC. Polymer 2004; in press.
[19] Wu HD, Ma CCM, Lee MS, Su YF, Wu YD. Compos Part A: Appl Sci Manuf 1997;28A:895.
[20] Fox TG. Bull Am Phys Soc 1956;2:123.
[21] Kwei TK. J Polym Lett Ed 1984;22:307.
[22] Kuo SW, Chang FC. Macromolecules 2001;34:4089.
[23] Coleman MM, Graf JF, Painter PC. Specific interactions and the miscibility of polymer blends. Lancaster: Technomic Publishing; 1991.
[24] Moskala EJ, Varnell DF, Coleman MM. Polymer 1985;26:228.
[25] Cortazar M, Pomposo JA. Macromolecules 1994;27:252.
[26] Serman CJ, Painter PC, Coleman MM. Polymer 1991;32:1049.
[27] McBrierty VJ, Douglass DC. J Polym Sci Macromol Rev 1981;16: 295.
[28] Demco DE, Johansson A, Tegenfeldt J. Solid State Nucl Magn Reson 1995;4:13.
[29] Clauss J, Schmidt-Rohr KWH. Acta Polym 1993;44:1.
[30] Martter TD, Foster MD, Ohno K, Haddleton DM. J Polym Sci Part B: Polym Phys 2001;40:1704.